

# Local Polymer Dynamics in Polymer—C<sub>60</sub> Mixtures

Jamie M. Kropka,<sup>†</sup> Victoria Garcia Sakai,<sup>‡,§</sup> and Peter F. Green<sup>\*,||</sup>

*Department of Chemical Engineering, The University of Texas at Austin, Austin, Texas 78712, NIST Center for Neutron Research, National Institute of Standards and Technology, Gaithersburg, Maryland 20899, Department of Materials Science and Engineering, University of Maryland, College Park, Maryland 20742, and Department of Materials Science, Applied Physics, University of Michigan, Ann Arbor, Michigan 48109*

Received November 15, 2007; Revised Manuscript Received January 21, 2008

## ABSTRACT

The complexity of intermolecular interactions in polymer–nanoparticle systems leads to spatial variations in structure and dynamics at both the meso- and nanoscale. Much of this behavior is manifested in properties such as the glass transition and the viscosity. Incoherent neutron scattering measurements of C<sub>60</sub>–polymer mixtures reveal that local polymer chain backbone motions in the glassy state are suppressed relative to those of the pure polymer. Moreover, the scattering spectrum of the melt suggests that the influence of C<sub>60</sub> on polymer dynamics is limited to the vicinity of the particles at nanosecond time scales. A model is presented to reconcile these observations with the bulk dynamical properties exhibited by the mixtures.

Very small concentrations of nanoparticles, on the order of a percent, can significantly alter the phase behavior and the mechanical and electrical characteristics of polymeric materials. Insight into how nanoparticles influence the associated morphological structure<sup>1–3</sup> and system dynamics<sup>4–6</sup> of polymer–nanoparticle mixtures is only beginning to emerge, and the advancement of knowledge in these areas will be key to developing design rules to engineer materials with desired properties.

The complexity of interactions, polymer–particle, polymer–polymer and particle–particle, that determine the properties exhibited by polymer-based nanocomposites (PNCs) manifest a diverse range of effects on polymer dynamics. For example, dynamic mechanical measurements show that PNCs containing silica particles exhibit two glass transition temperatures ( $T_g$ s).<sup>7</sup> Specifically, the particles are believed to induce two distinct regions of reduced polymer mobility near the particle surfaces: (1) chain segments tightly bound to the particle surfaces that do not relax over the experimental time scales and (2) loosely bound chains that give rise to an

additional, higher,  $T_g$  when the particles are sufficiently close and the loosely bound chains around many particles overlap. Other investigations of PNCs reveal only a single  $T_g$  that is shifted due to the influence of nanoparticles.<sup>5,8–11</sup> Particle-induced regions of altered polymer mobility are also suggested to underlie the  $T_g$  shifts in these materials. On the other hand, other PNC materials exhibit no change in the local dynamics associated with the  $T_g$ , while long-range motions of the chains are highly restricted.<sup>12</sup> Clearly, the effects of nanoparticles on polymer dynamics in each of these systems differ, and understanding the mechanism of influence is essential to discerning why this is the case.

Molecular dynamics (MD) simulations of PNCs reveal that changes in monomer packing near the polymer–particle interface lead to the formation of “shells” of perturbed polymer density around a nanoparticle which exhibit dynamics that differ from those of the neat polymer.<sup>13,14</sup> These simulations further suggest that such dynamical heterogeneities can provide a rationale for the observed changes in  $T_g$  and viscosity in the PNCs.<sup>13–15</sup> The common conclusion that can be drawn from all the aforementioned experimental and simulated observations is that an understanding of the microscopic dynamics in PNCs is key to understanding material property enhancements (by “microscopic” here, we mean the length scale of a few bonds).

Neutron scattering measurements offer the unique possibility of analyzing the spatial dimensions of atomic

\* Corresponding author. E-mail: pfgreen@umich.edu.

<sup>†</sup> Department of Chemical Engineering, The University of Texas at Austin.

<sup>‡</sup> NIST Center for Neutron Research, National Institute of Standards and Technology and Department of Materials Science and Engineering, University of Maryland.

<sup>§</sup> Current address: ISIS Facility, The Rutherford Appleton Laboratory, Chilton, Didcot, OX11 0QX, U.K.

<sup>||</sup> Department of Materials Science, Applied Physics, University of Michigan.

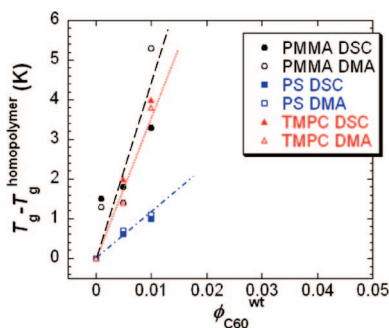


**Figure 1.** The change in glass transition temperature from that of the neat polymer as a function of  $C_{60}$  concentration. The dotted lines are a guide to the eye.

processes in their development over time and provide an excellent means of evaluating the microscopic dynamics of interest in PNCs.<sup>16,17</sup> In this paper, we use incoherent elastic neutron scattering (IENS) to examine three  $C_{60}$ -polymer PNCs:  $C_{60}$ -polystyrene (PS),  $C_{60}$ -poly(methyl methacrylate) (PMMA), and  $C_{60}$ -tetramethylbisphenol-A polycarbonate (TMPC). These materials exhibit an increase in their “bulk”  $T_g$ , as measured by differential scanning calorimetry and dynamic mechanical analysis, as depicted in Figure 1. Here, we will demonstrate that insight into the mechanism by which  $C_{60}$  increases the  $T_g$  can be gained from IENS measurements of the materials in the glassy state. Further, mechanical measurements of these PNCs show no evidence of excess structural or dynamic heterogeneity relative to the neat polymer and suggest that the effect of the particles may be described in terms of an increased segmental friction coefficient for the polymer.<sup>11</sup> However, quasi-elastic neutron scattering (QENS) measurements reveal that the influence of  $C_{60}$  on polymer melt dynamics is limited to the vicinity of the particle surfaces at the nanosecond time scale. We use this finding to explain how the increases in the longest relaxation time of the polymer,  $\tau_R$ , can be reconciled with a mechanism involving transient polymer segment-particle interactions.

The  $C_{60}$ -polymer PNCs were made via a solution-dissolution/solvent-evaporation method. The  $C_{60}$  (Alpha Aesar,<sup>18</sup> 99+ %) was added to organic solvents and sonicated (Sonicor, SC-40) for 15 min to disperse the fullerenes into solution. PMMA (Pressure Chemical;  $M_w = 254.7$  kg/mol,  $M_w/M_n = 1.15$ ), PS (Pressure Chemical;  $M_w = 152$  kg/mol,  $M_w/M_n = 1.06$ ), and TMPC (Bayer;  $M_w = 37.9$  kg/mol,  $M_w/M_n = 2.75$ ) were also dissolved in organic solvents, and the nanoparticle and polymer solutions were mixed in proportion to create the appropriate nanocomposite concentration. Toluene was used to make the PMMA and PS samples, while 1,1,2,2-tetrachloroethane was used to make the TMPC samples. The solvent was evaporated from the mixtures at 348 K. Residual solvent was subsequently removed by drying the samples under high vacuum at 453 K for 15 h. The TMPC samples were further heated to 493 K for 30 min. We found that lower annealing temperatures were insufficient to completely remove residual solvent.

Aluminum boats containing the polymer samples were placed in an annular, thin-walled aluminum cell that was mounted on the High Flux Backscattering Spectrometer (HFBS)<sup>19</sup> on the NG2 beam line at the NIST Center for Neutron Research and cooled under vacuum. The spectrometer operated in two modes. The first was a fixed window mode (stationary Doppler drive), where the elastic intensity was recorded as the sample temperature,  $T$ , was increased from 50 K to 525 K at a rate of 1 K/min. The Doppler drive was also turned on to measure the QENS spectrum over a dynamic range of  $\pm 11 \mu\text{eV}$  and over temperatures spanning 375 K to 525 K. This is a limited dynamic range, but the elastic scans, as will be seen in the following, suggest that faster processes, such as methyl rotations, are unaffected by  $C_{60}$ . Hence, measurements that resolve faster processes would not provide further information on the influence of  $C_{60}$  on polymer dynamics. Mechanical measurements that resolve the influence of  $C_{60}$  on slower processes have also been reported for one of the PNCs in a previous publication.<sup>11</sup> Raw data were normalized to monitor and to the intensity at the lowest measured temperature. Mean-square atomic displacements (MSDs) and Fourier transforms of the QENS spectra were evaluated using software developed by NIST (Data Analysis and Visualization Environment).<sup>20</sup> For the evaluation of the QENS measurements, the resolution of the spectrometer was taken as the QENS spectrum of the sample at  $T < 5$  K.

The incoherent scattering cross section of hydrogen is approximately 20 times greater than the total scattering cross section of C or O and approximately 40 times greater than its own coherent scattering cross section. Hence, in the  $C_{60}$ -polymer PNCs examined, the scattering is dominated by the incoherent scattering of the hydrogen atoms of the polymers and only the dynamics of the polymers is probed.

We first discuss the polymer segmental dynamics, as determined from the incoherent elastic scattering intensity,  $I_{el}(T)$ . The focus of our attention will be on PNCs containing  $\phi_{C_{60}}^{wt} = 0.01$ ; the most significant changes in  $T_g$  and  $\tau_R$  occur at this concentration.  $C_{60}$  dispersion within each polymer host is qualitatively equivalent to that previously reported for PMMA;<sup>11</sup> micrographs which illustrate the  $C_{60}$  dispersion within the PS and TMPC hosts are included as Supporting Information. Figure 2 shows  $I_{el}$ , summed over the momentum transfer range  $0.25 \text{ \AA}^{-1} \leq Q \leq 1.75 \text{ \AA}^{-1}$ , plotted as a function of  $T$  for the neat polymers and the PNCs. In general, both Debye-Waller decay and anharmonic local segmental motions active in the time scale of the elastic window can contribute to the decrease in  $I_{el}$  with  $T$  for the polymers at  $T < T_g$ . In Figure 2a,  $\ln[I_{el}]$  decreases linearly with  $T$  for PS, in a manner consistent with Debye-Waller predictions, up to the calorimetric  $T_g$  of the material. On the other hand, plots of  $\ln[I_{el}]$  versus  $T$  show nonlinearities for both PMMA (Figure 2b) and TMPC (Figure 2c) for  $T < T_g$ . The nonlinearities can be attributed to methyl rotations ( $T \approx 50$  K to 100 K) and localized chain backbone motions<sup>21</sup> ( $T \approx 200$  K to 350 K) entering the elastic window of the spectrometer. All materials show a large drop in  $I_{el}$  near the calorimetric  $T_g$ .

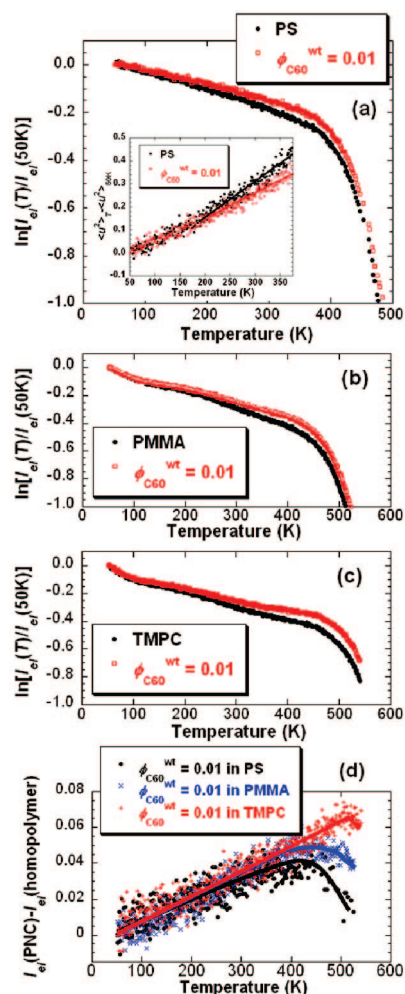


**Figure 2.** The decrease in the elastic scattering intensity as a function of temperature for (a) PS and  $\varphi_{C_{60}}^{wt} = 0.01$  in PS, (b) PMMA and  $\varphi_{C_{60}}^{wt} = 0.01$  in PMMA, and (c) TMPC and  $\varphi_{C_{60}}^{wt} = 0.01$  in TMPC. The inset of (a) depicts the relationship between MSD and temperature described in the text. The difference between the elastic scattering intensity of the PNCs and neat polymers is given as a function of temperature in (d). The solid lines are a guide to the eye.

$I_{el}$  is increased for all PNCs relative to their homopolymer analogues, revealing a decrease in atomic motions of the polymer chain segments upon the addition of  $C_{60}$ . The increase in  $I_{el}$  is observed over a very broad temperature range and cannot be explained solely by the increase in  $T_g$  for the composites; i.e., rescaling the  $x$ -axes in panels a–c of Figure 2 to  $(T - T_g)/T_g$  will not result in a collapse of the PNC and neat polymer data. For PS, the decrease in the slope of  $\ln[I_{el}]$  versus  $T$ , for  $T < T_g$ , upon  $C_{60}$  addition is indicative of a restriction of harmonic vibrations. For the PMMA and TMPC PNCs, the drop in  $I_{el}$  due to methyl rotations (at  $T \approx 50$  K to 100 K) is unchanged from that of the neat polymers, indicating that the methyl rotations in the materials are unaffected by the  $C_{60}$  particles. At higher  $T$ , however, a suppression of the intensity drop associated with local backbone motions leads to an increase in  $I_{el}$  for the PMMA and TMPC PNCs relative to the neat polymers.

Figure 2d presents the difference between the elastic scattering intensities for the PNCs and the pure polymers,

$[I_{el}(PNC) - I_{el}(\text{homopolymer})]$ , as a function of temperature. Interestingly, all the data superpose at low  $T$  and reach a peak that is positioned relative to the calorimetric  $T_g$  of the pure polymer. The superposition of the data indicates that the magnitude of the suppression of polymer dynamics in the glassy state, due to the  $C_{60}$  influence, is comparable for all systems. To further characterize the glassy behavior, we evaluate the MSD,  $\langle u^2 \rangle$ , of the materials using a linear fit of  $\ln I_{el}$  vs  $Q^2$  in the Debye–Waller approximation<sup>16,17</sup>

$$\ln I_{el} \propto \left(-\frac{1}{3} Q^2 \langle u^2 \rangle\right) \quad (1)$$

The resulting MSD for PS and the PS– $C_{60}$  PNC (evaluated for  $0.38 \text{ \AA}^{-2} < Q^2 < 2.56 \text{ \AA}^{-2}$ ) is plotted in the inset of Figure 2a. The behavior of the other polymer systems is similar, but methyl rotations that enter the time window of the spectrometer influence the relationship between  $\langle u^2 \rangle$  and  $T$ , even at  $T$  as low as 50 K, and obscure the following analysis. Hence, we focus our attention on the PS materials.

We first note an observation that was not apparent from inspection of the  $I_{el}$  data; PS does not exhibit harmonic behavior above 200 K. For  $T < 200$  K, both PS and the PS– $C_{60}$  PNC exhibit equivalent  $\langle u^2 \rangle$ ; the linear dependence of  $\langle u^2 \rangle$  on  $T$  enables a determination of the harmonic force constant of the materials,  $\kappa \approx 3k_B T / \langle u^2 \rangle$ , which is also equivalent for the pure polymer and composite. For  $T > 200$  K, the PS  $\langle u^2 \rangle$  exhibits a stronger dependence on  $T$  and exceeds that of the composite. Although the harmonic approximation is not strictly valid in this regime, the  $T$  dependence of  $\langle u^2 \rangle$  for 200 K  $< T < 350$  K can be well described by a linear fit for both the neat polymer and composite. The determination of a force constant within this temperature range,  $\kappa^{200-350K}$ , provides a means to evaluate the restriction of the relaxation process associated with local polymer chain backbone motions due to the addition of  $C_{60}$ . This analysis yields an effective local “stiffness”<sup>22</sup> of the material and estimates an increase in  $\kappa^{200-350K}$  of 24% for the composite relative to the neat polymer.

The suppression of the local relaxation dynamics of the composite is consistent with an enhancement of cohesive interactions in the system, which may be the root of the increase in  $T_g$  for the PNCs; i.e., the system must acquire more thermal energy before polymer segments can overcome local energy barriers and thereby enable polymer center-of-mass motions. It has even been proposed that the local segmental relaxation processes restricted in the composite are associated with the short-time regime of the  $\alpha$ -relaxation.<sup>21</sup> MD simulations of polymer melts by Smith et al.<sup>23</sup> have suggested that both increased polymer segment packing densities and the energy topography of a surface can lead to stronger caging of polymer segments near an attractive surface. Our results indicate that  $C_{60}$  induces similar effects in the glassy state of the polymers investigated and that the effects can be discerned from the bulk IENS measurements.

Each curve in Figure 2d exhibits a maximum at  $\approx 50$  K above the neat polymer calorimetric  $T_g$ . The decrease of  $[I_{el}(PNC) - I_{el}(\text{homopolymer})]$  for  $T > T_g + 50$  K is consistent with the PNC melt density and relaxation dynamics homogenization toward that of the pure polymer with

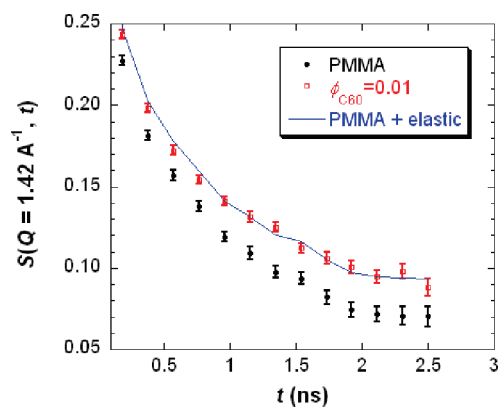


**Figure 3.** Intermediate scattering function for PMMA and the  $\varphi_{C_{60}}^{wt} = 0.01$  in PMMA PNC at  $Q = 1.42 \text{ \AA}^{-1}$  and  $T = 525 \text{ K}$ . The solid line represents the PMMA data corrected for an elastic contribution according to eq 2 with  $\alpha = 0.025$ .

increasing temperature found in MD simulations.<sup>13</sup> It is noteworthy that the absence of a “kink” in the  $I_{el}$  versus  $T$  data for the PNCs at  $T > T_g$  suggests that the decrease of  $[I_{el}(\text{PNC}) - I_{el}(\text{homopolymer})]$  is not due to the sudden onset of diffusive motions associated with a fraction of polymers strongly influenced by the particle surfaces.<sup>7</sup> Rather, we suggest that a transient immobilization of polymer segments at the particle surfaces becomes less significant at higher  $T$ , as nearest neighbor distances increase and weaken the polymer–particle interactions relative to the thermal energy of the system.

To further explore this last suggestion, we consider the melt dynamics of the PNCs. The increased  $I_{el}$  for the PNCs in the melt ( $T > T_g$ ) could be due to either of two effects: (1) a “permanent” adsorption of polymer segments to the particle surface that immobilizes the adsorbed atoms over long time scales or (2) a transient immobilization of the polymer segments closest to the particle surface, which may slowly exchange locations with segments from neighboring chains. In the former, the dynamics of only a fraction of the polymer segments are affected by the particles, and the bulk of the polymer remains unaffected. This appears not to be the case in the  $C_{60}$  PNCs, as our measurements show an increase in the bulk  $T_g$  of the PNCs (Figure 1). Moreover, mechanical rheological measurements of the PMMA– $C_{60}$  PNCs reveal an increase in the longest relaxation time that is not consistent with a permanent immobilization of only a fraction of polymer chains.<sup>11</sup> We argue that the latter description of a transient segmental immobilization is a more appropriate description of the behavior of the  $C_{60}$  PNCs.

Immobilization of polymer segments at the particle surface over nanosecond time scales is supported by the QENS data. To illustrate this, we evaluate the intermediate scattering function,  $S(Q, t)$ , for the PMMA samples at a melt temperature of 525 K in Figure 3. Figure 3 reveals an increase in  $S(Q, t)$  for the PNC relative to the pure polymer over the entire resolvable time scale. In fact, the  $S(Q, t)$  data of PMMA can be well fit to the  $S(Q, t)$  data of PMMA– $C_{60}$  by adding an elastic contribution according to the following relationship

$$S(Q, t)_{\text{PMMA-C}_{60}} = \alpha + (1 - \alpha)S(Q, t)_{\text{PMMA}} \quad (2)$$

where  $\alpha = 0.025$  represents the fraction of immobilized polymer chain segments. This relation holds over the entire  $Q$  range measured by the HFBS. Hence, we attribute the difference between the pure polymer and PNC  $S(Q, t)$  to the immobilization of polymer segments at the polymer–particle interfaces over nanosecond time scales; all other polymer segments retain homopolymer-like dynamics. This finding is similar to observations in PDMS–silica mixtures.<sup>24</sup> The time scale associated with immobilization of the chain segments at the  $C_{60}$  surfaces, however, must be much less than the longest relaxation time of the polymer chains. In this case, the local influence of the particles can be felt by many polymer segments throughout the time scale of the longest relaxation. Consequently the increases in  $\tau_R$  measured via rheology can be described by an increase in the local friction experienced by the chain.<sup>11</sup> We note that the relative dependence of  $\alpha$  on  $T$  can be resolved from Figure 2d, as  $[I_{el}(\text{PNC}) - I_{el}(\text{homopolymer})]$  is proportional to  $\alpha$ .

Another way to interpret the increase in  $T_g$  for the  $C_{60}$  PNCs may be understood in terms of the dynamic percolation model of Long and Lequeux.<sup>25</sup> In this model the dynamics of a melt are characterized by the existence of “fast” and “slow” domains, associated with density fluctuations in the system. Percolation of the “slow” domains occurs upon decreasing the temperature and is associated with the glass transition. The presence of immobilized polymer segments at the particle surfaces increases the fraction of “slow” domains in the PNC relative to the neat polymer; the enhancement in the fraction of slow domains in the PNC will induce their percolation at a higher temperature relative to the neat polymer and result in an increase in  $T_g$  for the PNC.

In summary, we have shown that the effect of adding  $C_{60}$  to three different polymer hosts, PS, PMMA, and TMPC, is to suppress the polymer segmental dynamics in all cases. Specifically, the local polymer chain backbone motions in the PNCs are suppressed relative to those of the neat polymer, which likely plays a role in the observed increases in  $T_g$  of the materials. In the melt, the dynamics of the polymer segments in the vicinity of the particle surfaces are suppressed relative to the neat polymer, and this effect results in an excess elastic fraction of polymer segments at the nanosecond time scale. The elastic fraction diminishes as the temperature is increased above  $T_g + 50 \text{ K}$ . These results suggest that effects on polymer dynamics that are limited to the vicinity of particle surfaces at the nanosecond time scale can account for changes in bulk dynamics resolved with mechanical measurements.

**Acknowledgment.** Support for this research from the National Science Foundation #DMR 0601890 and from the US Department of Energy DOE#DE-FG02-07ER46412 is gratefully acknowledged. The facilities at NIST were supported in part by the National Science Foundation under Agreement No. DMR-0454672.

**Supporting Information Available:** Micrographs which depict the  $C_{60}$  dispersion within the PS and TMPC hosts. This material is available free of charge via the Internet at <http://pubs.acs.org>.

## References

- (1) Thompson, R. B.; Ginzburg, V. V.; Matsen, M. W.; Balazs, A. C. *Science (Washington, DC, U.S.)* **2001**, 292 (5526), 2469–2472.
- (2) Mackay, M. E.; Tuteja, A.; Duxbury, P. M.; Hawker, C. J.; Van Horn, B.; Guan, Z.; Chen, G.; Krishnan, R. S. *Science (Washington, DC, U.S.)* **2006**, 311 (5768), 1740–1743.
- (3) Warren, S. C.; DiSalvo, F. J.; Wiesner, U. *Nat. Mater.* **2007**, 6 (2), 156–161.
- (4) Mackay, M. E.; Dao, T. T.; Tuteja, A.; Ho, D. L.; Van Horn, B.; Kim, H.-C.; Hawker, C. J. *Nat. Mater.* **2003**, 2 (11), 762–766.
- (5) Bansal, A.; Yang, H.; Li, C.; Cho, K.; Benicewicz, B. C.; Kumar, S. K.; Schadler, L. S. *Nat. Mater.* **2005**, 4 (9), 693–698.
- (6) Narayanan, R. A.; Thiyagarajan, P.; Lewis, S.; Bansal, A.; Schadler, L. S.; Lurio, L. B. *Phys. Rev. Lett.* **2006**, 97 (7), 075505/1–075505/4.
- (7) Tzagaropoulos, G.; Eisenburg, A. *Macromolecules* **1995**, 28 (1), 396–8.
- (8) Becker, C.; Krug, H.; Schmidt, H. Better Ceramics through Chemistry VII: Organic/Inorganic Hybrid Materials. *Mater. Res. Soc. Symp. Proc.* **1996**, 435, 237–242.
- (9) Ash, B. J.; Siegel, R. W.; Schadler, L. S. *J. Polym. Sci., Part B: Polym. Phys.* **2004**, 42 (23), 4371–4383.
- (10) Rittigstein, P.; Torkelson, J. M. *J. Polym. Sci., Part B: Polym. Phys.* **2006**, 44 (20), 2935–2943.
- (11) Kropka, J. M.; Putz, K. W.; Pryamitsyn, V.; Ganesan, V.; Green, P. F. *Macromolecules* **2007**, 40 (15), 5424–5432.
- (12) Du, F.; Scogna, R. C.; Zhou, W.; Brand, S.; Fischer, J. E.; Winey, K. I. *Macromolecules* **2004**, 37 (24), 9048–9055.
- (13) Starr, F. W.; Schroder, T. B.; Glotzer, S. C. *Phys. Rev. E* **2001**, 64, 021802.
- (14) Smith, G. D.; Bedrov, D.; Li, L.; Bytner, O. *J. Chem. Phys.* **2002**, 117, 9478–9489.
- (15) Pryamitsyn, V.; Ganesan, V. *Macromolecules* **2006**, 39 (2), 844–856.
- (16) Frick, B.; Richter, D. *Science (Washington, DC, U.S.)* **1995**, 267 (5206), 1939–45.
- (17) Soles, C. L.; Douglas, J. F.; Wu, W. I.; Dimeo, R. M. *Phys. Rev. Lett.* **2002**, 88 (3), 037401/1–037401/4.
- (18) The use of commercial products identified in this paper does not imply recommendation or endorsement by the National Institute of Standards and Technology, nor does it imply that the materials or equipment identified are necessarily the best available for the purpose.
- (19) Meyer, A.; Dimeo, R. M.; Gehring, P. M.; Neumann, D. A. *Rev. Sci. Instrum.* **2003**, 74, 2759–2777.
- (20) <http://www.ncnr.nist.gov/dave>.
- (21) Colmenero, J.; Arbe, A. *Phys. Rev. B: Condens. Matter Mater. Phys.* **1998**, 57 (21), 13508–13513.
- (22) Riggleman, R. A.; Douglas, J. F.; de Pablo, J. J. *J. Chem. Phys.* **2007**, 126 (23), 234903.
- (23) Smith, G. D.; Bedrov, D.; Borodin, O. *Phys. Rev. Lett.* **2003**, 90 (22), 226103/1–226103/4.
- (24) Arrighi, V.; Higgins, J. S.; Burgess, A. N.; Floudas, G. *Polymer* **1998**, 39 (25), 6369–6376.
- (25) Long, D.; Lequeux, F. *Eur. Phys. J. E: Soft Matter* **2001**, 4 (3), 371–387.

NL072980S